



# Miscibility and interactions in chitosan acetate/poly(N-vinylpyrrolidone) blends

Katarzyna Lewandowska\*

Nicolaus Copernicus University, Faculty of Chemistry, Chair of Chemistry and Photochemistry of Polymers, 7 Gagarin Street, 87-100 Torun, Poland

## ARTICLE INFO

### Article history:

Received 18 August 2010

Received in revised form 11 January 2011

Accepted 26 January 2011

Available online 17 February 2011

### Keywords:

Poly(N-vinylpyrrolidone)

Chitosan

Polymer blends

Miscibility

## ABSTRACT

In the present study, the blends of chitosan (Ch) and poly(N-vinylpyrrolidone) (PVP) were investigated by differential scanning calorimetry (DSC), dynamic mechanical analysis (DMA), Fourier transform infrared spectroscopy (FTIR) and wide angle X-ray diffraction (WAXD). WAXD patterns of homopolymers and their blends indicated that blending of amorphous materials, such as PVP, with semicrystalline polymer, such as chitosan gives rise to an amorphous structure. From thermal curves the glass transitions temperature have been determined and compared. The thermal results indicated that in the solid ChA/PVP blends the components are poorly miscible. The FTIR spectra of film blends, in the carbonyl stretching region of PVP and the hydroxyl stretching bands of chitosan have been analyzed. The observed shift of these bands and the change of their shape depends on (I) the blend composition, on (II) the chemical structure of chitosan {chitosan in its amine form (Ch) or chitosan acetate (ChA)}, and on (III) the molecular weight of PVP, whereas the influence of temperature in the range of 298–403 K seems to be negligible.

© 2011 Elsevier B.V. All rights reserved.

## 1. Introduction

Water soluble polymers are important from an industrial viewpoint. In general, it is convenient to divide them into three groups according to their origin, i.e. natural, modified natural (semisynthetic) and synthetic [1]. They are used in several applications as, e.g. in the food processing industry, paints, medicine and pharmacy. An important water soluble polymer is poly(N-vinylpyrrolidone) (PVP). PVP is a synthetic, non-ionic polymer soluble in water and many organic liquids. PVP repeating unit contains a highly polar amide group, which determines its hydrophilic and polar-attracting properties and apolar methylene and methine groups, which confer to PVP the hydrophobic properties. This polymer is classified as a polar aprotic polymer [2]. PVP is physiologically inactive. Its great adsorptive and complexing ability towards different types of small-molecular substances has led to the application of PVP in medicine, pharmacy, food processing, cosmetics etc. [2].

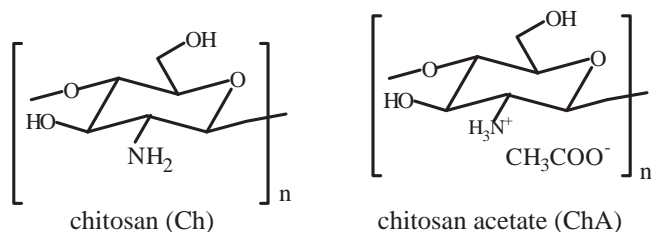
Chitosan (Ch)-poly[ $\beta$ -(1 $\rightarrow$ 4)-2-amino-2-deoxy-D-glucopyranose] is the principal derivative of chitin [3]. This polymer is produced by alkaline deacetylation of chitin. Chitin, after cellulose, is the most widespread polymer in nature, its insolubility, however, makes impossible further processing. Chitosan is readily soluble in dilute inorganic and organic acids. Chitosan gives water-soluble salts with acetic acid (Scheme 1). Specific properties of chitosan such as bioactivity, biocompatibility and biodegradability have resulted in an increasing interest of its

investigation and application, e.g. in medicine, pharmacy and food and cosmetic industries.

Well established polymer/polymer blending is an important method to improve the original properties of one or both components. Theoretically, it has become clear that the miscibility of polymer blends is mainly determined by the chemical structure, composition and molecular weight of each component [4]. The polymers with relatively low molecular weight tend to be more miscible. It is also important to relate the chemical structure of polymers to their physical properties, as miscibility is often a result of specific interaction between two polymeric components, such as hydrogen bonding, donor–acceptor, ionic, dipole–dipole, charge transfer type, etc. The presence of strong intermolecular force especially hydrogen bond may result in different physico-chemical characteristics compared to the initial polymers [4]. The various techniques have been used to characterize the miscibility of polymer blends, such as optical transparency, FTIR, DSC, DMA and high-resolution solid state  $^{13}\text{C}$  NMR spectroscopy. The properties of the blends of naturally occurring polysaccharides such as cellulose, chitin, chitosan and starch with synthetic polymers have been investigated [5–7]. The miscibility of chitosan with PVP has also been presented [8–15]. Thermal properties of ChA/PVP blends showed a single glass transition [10–12]. NMR and FTIR analyses proved that hydrogen bonding was present between the chitosan and PVP [9,11,13–15]. WAXD measurements suggested that the miscibility of ChA with PVP sets in amorphous regions [8,12,13]. However, the authors of these studies [8–15] did not frequently give full characteristics of the used polymer samples. Thus, some interesting aspect still remains to be elucidated such as the influence of the molecular weight of polymeric components or the degree

\* Corresponding author.

E-mail address: [reol@chem.uni.torun.pl](mailto:reol@chem.uni.torun.pl)



**Scheme 1.** The chemical structure of chitosan and chitosan acetate.

of deacetylation of chitosan on the miscibility in the chitosan/PVP blends.

The purpose of this paper is the evaluation of the miscibility of poly(*N*-vinylpyrrolidone) differing in molecular weight with chitosan acetate (ChA) or chitosan (Ch) with relatively low deacetylation degree on the basis of differential scanning calorimetry (Hyper DSC), dynamic mechanical thermal analysis (DMA), Fourier transform infrared spectroscopy (FTIR) and wide angle X-ray diffraction (WAXD). The influence of temperature on the hydrogen bond of ChA/PVP blends in FTIR study has been discussed.

## 2. Experimental

### 2.1. Materials

The characteristics of chitosan (Ch) and poly(*N*-vinylpyrrolidone) (PVP) samples are given in Table 1. Distilled water and 0.1 M aqueous acetic acid were used as solvent.

The viscosity average molecular weight  $\bar{M}_v$  of chitosan and PVP was measured with an Ubbelohde viscometer. The temperature of viscosity measurement, the solvent and Mark–Houwink–Sakurada constants  $K$  and  $a$  for evaluating  $\bar{M}_v$  are specified in Table 1.

The degree of deacetylation (DD) of chitosan was estimated according to Polish Standards (PN-87/A-86850).

### 2.2. Preparations

Chitosan and PVP were solubilised, separately, in 0.1 M aqueous acetic acid and then mixed at different weight ratios. The solution blends were poured on a glass plate covered with polyethylene film and evaporated at room temperature (298 K). Films of pure ChA and PVP were prepared in the same manner. The solid films were further dried at 323 K for 24 h under vacuum and stored in a desiccator. All films of blends cast from stable mixed polymer solutions were visually homogeneous irrespective of composition. For FTIR measurements the other series of films of chitosan acetate and mixtures were neutralized by immersing into a sodium hydroxide solution (1%) for 15 min. After the alkaline treatment, the films were rinsed and left in distilled water, overnight. After drying in air, films were stored in a desiccator.

**Table 1**  
Characteristics of polymer samples.

Polymer	$\bar{M}_v \times 10^{-3}$ (g/mol)	DD (%)	Source
Ch	471 <sup>a,c</sup>	83 <sup>a</sup>	Institute of Sea Fisher (Poland)
PVP I	930 <sup>a,d</sup> , 360 <sup>b</sup>		Sigma Chemical Company (USA)
PVP II	22 <sup>a,e</sup> , 25–30 <sup>b</sup>		Merck (England)

$\bar{M}_v$  is the viscosity average molecular weight, DD is the degree of deacetylation of chitosan.

<sup>a</sup> Determined in this study.

<sup>b</sup> Producer's value.

<sup>c</sup>  $K = 1.81 \times 10^{-2}$  dl/g,  $a = 0.93$ ,  $T = 298$  K, solvent: 0.1 M  $\text{CH}_3\text{COOH}/0.2$  M NaCl [16].

<sup>d</sup>  $K = 3.93 \times 10^{-4}$  dl/g,  $a = 0.59$ ,  $T = 303$  K, solvent: water [17].

<sup>e</sup>  $K = 6.74 \times 10^{-3}$  dl/g,  $a = 0.55$ ,  $T = 298$  K, solvent: water [18].

### 2.3. DSC measurements

The calorimetry measurements were made on ca. 2 mg samples with a Perkin Elmer Pyris Diamond apparatus with the power compensation using DSC technique: high speed DSC (Hyper DSC) [19–21]. Hyper DSC technique with fast scanning rates enabling increased sensitivity and high throughput has recently been introduced by Perkin Elmer. With very fast temperature scanning rates (100–500 °C/min) in heating as well as on cooling over a broad temperature range, sensitivity and throughput have dramatically increased by a factor of ten over most conventional DSC analyses. Due to the fast scanning rate, the re-crystallization during melting, decomposition after melting, and unknown thermal behaviour are either completely eliminated or significantly reduced by this method. The temperature readings were calibrated with an indium standard. The DSC curves of samples under helium atmosphere were recorded at heating rate of 300 °C/min in two scans between –20 °C and 250 °C (253–523 K). In the first cycle, the amounts of solvent and/or water were eliminated and thermal histories of the respective samples were equalized completely. Then the scans were run from –20 °C to 250 °C to record stable thermograms. The reported  $T_g$  are those from the second scan.

### 2.4. DMA measurements

Dynamic mechanical thermal analysis (DMA) was carried out using a Polymer Laboratories DMTA Mk III analyser. Samples were tested by bending mode and tensile mode, at a frequency of 1 Hz in the range of –20 °C to 250 °C (223–523 K) and heating rate of 5 °C/min. In the DMA instrument a film sample is longitudinally deformed by a small sinusoidal stress. The resulting strain, which lags behind the applied force by a phase angle  $\delta$ , is measured. The values of storage modulus  $E'$  (in-phase component), the loss modulus  $E''$  (out-of-phase component) and bending loss tangent  $\tan \delta = E''/E'$  were obtained.

### 2.5. FTIR analysis

FTIR spectrum was recorded on a Perkin Elmer Spectrum 2000, in the wavenumber range between 4000 and 400  $\text{cm}^{-1}$ , resolution of 2  $\text{cm}^{-1}$  and 60 times scanning. The oven temperature controller had an accuracy of  $\pm 1$  °C.

### 2.6. WAXD

X-ray diffractograms were recorded by means of HZG-4 X-ray diffractometer with Ni-filtered  $\text{CuK}\alpha$  radiation generated at 30 kV and 20 mA. The scan was taken in the  $2\theta$  range of 4–50° with step size of 0.1°. Crystallinity was determined by integration of the areas under the curves.

Crystallinity  $X_c$  of the films was calculated by using the relation:

$$X_c = \frac{F_c}{F_c + F_a} \times 100\%$$

where  $F_c$  and  $F_a$  is the area of crystal and noncrystal regions, respectively.

## 3. Results and discussion

### 3.1. DSC

The results of DSC measurements carried out for ChA/PVP cast films are shown in Fig. 1 and Table 2. Each curve (Fig. 1) was shifted in relation to the other to facilitate the presentation of the results. The homopolymer PVP showed  $T_g$  at 174 °C (447 K) and at 146 °C

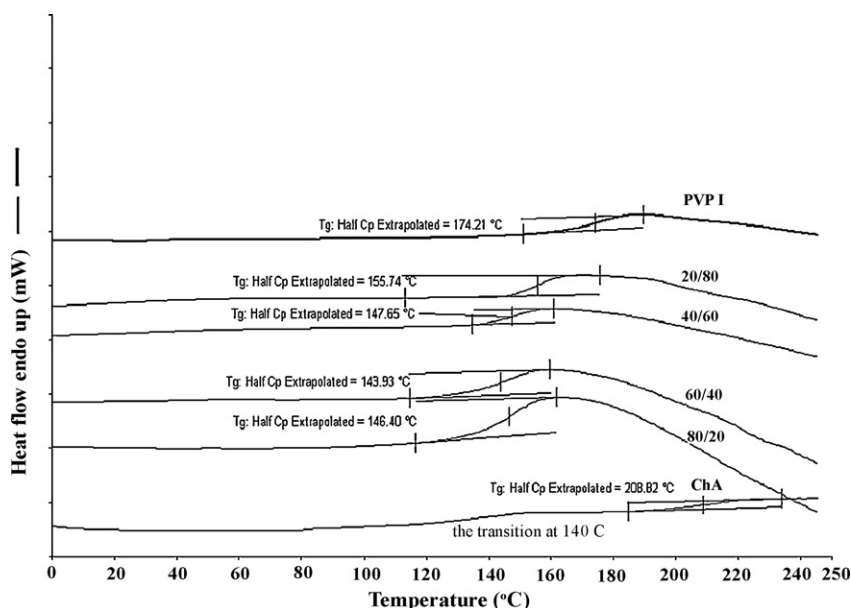


Fig. 1. DSC curves for ChA, PVP I and their blends.

(419 K) for PVP I and PVP II, respectively. The differences in the observed  $T_g$  values are due to the different molecular weight of PVP samples. The influence of  $\bar{M}$  on  $T_g$  for PVP was observed also by Turner and Schwartz [22].

As was shown in our earlier DSC measurements, ChA showed two transitions: the first one, more pronounced broad relaxation is situated at about 140 °C (413 K) and the second transition, weak, is observed at about 209 °C (482 K) [21]. The transition at about 140 °C (413 K) is assumed to be connected with the local motions within the amine groups in chitosan [21,23], while that at about 209 °C (482 K) we considered as the glass transition of chitosan [21]. In the ChA/PVP I and ChA/PVP II system blends only the first transitions is observed (Fig. 1). In both systems the transition temperature is situated closer to the temperature of the local motions within the amine groups in chitosan, and in the case of ChA/PVP II blends it practically covers the  $T_g$  values of PVP II (Table 2). The transitions are broad, which indicates an increase in microheterogeneity of the samples. The results in Table 2 also show that only the ChA/PVP I blends at  $w_{\text{ChA}} > 0.5$  presented a shift of the transition temperature to higher values, closer to the  $T_g$  of PVP I. These results suggest that in the investigated solid ChA/PVP blends the components are poorly or not miscible. Moreover, for the blends with  $w_{\text{ChA}} \geq 0.6$ , the

down turn in the heat flow is observed above 180 °C, which may be attributed to the beginning of degradation of samples. These results indicate a reduction in thermal stability of homopolymers in the mixtures, especially the higher content of ChA in polymer blends. This conclusion needs additional measurements, e.g. TG analysis.

Presented results are in contradiction with the DSC results of Sakurai et al. [12], who used chitosan sample with high deacetylation degree (DD = 96%), who not specified the molecular weight of chitosan and the type of molecular weight of PVP (only the value of  $\bar{M} = 9 \times 10^4$  is given), however their DSC results on ChA/PVP blends followed the theoretical curve of Fox [24]. It is striking that Sakurai et al. [12] in the DSC measurements did not observe the lower transition temperature situated at  $\sim 140$  °C, it is the temperature of local motions within the chitosan amine region, though their chitosan sample had high DD in comparison with the chitosan sample used in this paper.

### 3.2. DMA

The transition temperatures obtained in the DMA measurements of the investigated system are shown in Figs. 2–7. Fig. 2 shows the  $\tan \delta$  thermograms of PVP I and ChA, respectively. For PVP II sample, DMA curves were not obtained, because PVP II film is too fragile to perform DMA measurements using the bending mode.

Table 2  
The values of the transition temperature of ChA/PVP blends.

Blend composition	$T$ (°C)
ChA/PVP I	
100:0	140 ± 3
80:20	209 ± 2
60:40	146 ± 2
50:50	144 ± 2
40:60	142 ± 2
20:80	148 ± 1
0:100	156 ± 3
	174 ± 3
ChA/PVP II	
100:0	140 ± 3
80:20	209 ± 2
60:40	144 ± 1
50:50	144 ± 3
40:60	145 ± 1
20:80	143 ± 1
0:100	143 ± 3
	146 ± 3

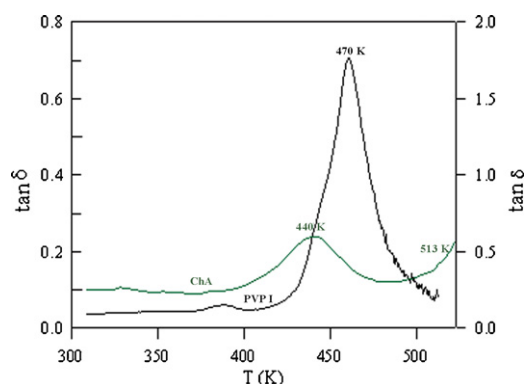
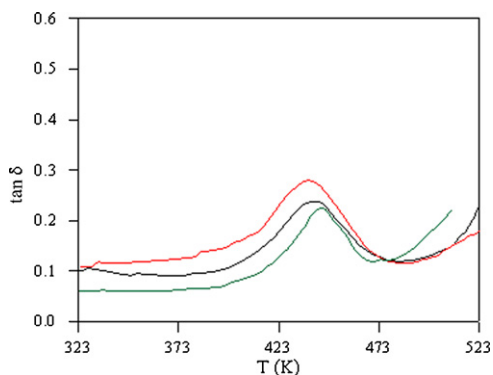
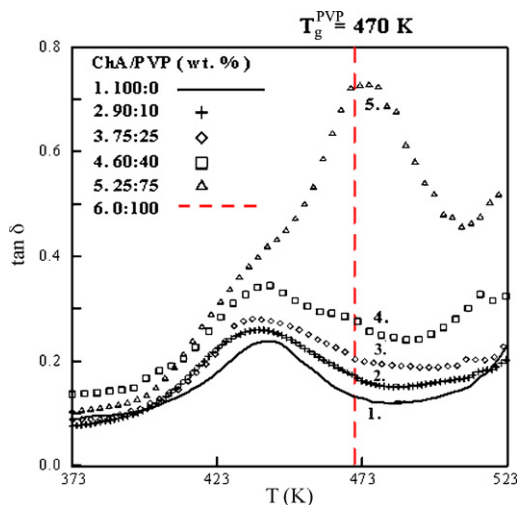


Fig. 2. The  $\tan \delta$  thermograms of ChA and PVP I (the bending mode).



**Fig. 3.** The  $\tan \delta$  thermograms of ChA (the bending mode). —: DD = 100% —: DD = 83% —: DD = 75%. (For interpretation of the references to color in this figure legend, the reader is referred to the web version of the article.)



**Fig. 4.** The  $\tan \delta$  thermograms of ChA, PVP I and ChA/PVP I blends (the bending mode).

As can be observed, the main difference between the curves of PVP and ChA is the magnitude of the transitions, which may be an indication of the difference in morphology of both homopolymers. PVP is an amorphous polymer, and its glass transition peak

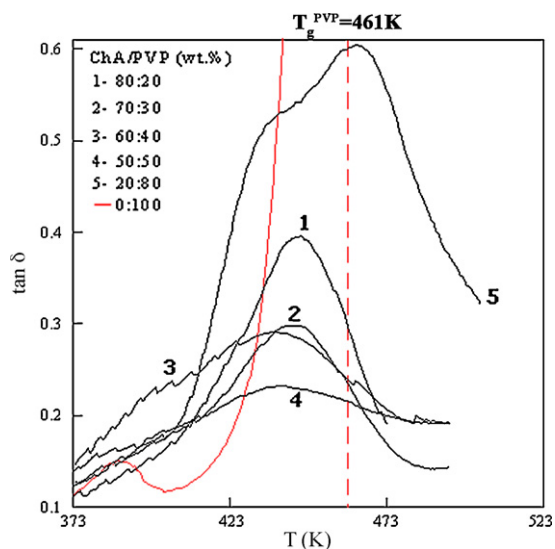


**Fig. 5.** The  $\tan \delta$  thermograms of ChA, PVP I, and their blends (tensile mode).

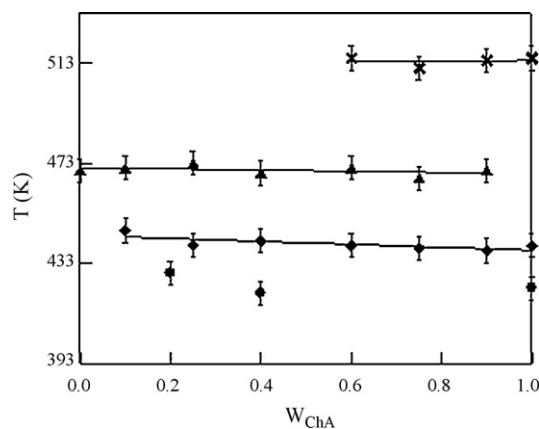


**Fig. 6.** The transition temperatures of ChA, PVP I and ChA/PVP I blends found in DMA measurements (bending mode). (♦) The transition temperature in the amine region of ChA, (x)  $T_g^{\text{ChA}}$  and (▲)  $T_g^{\text{PVP}}$ . (●) The transition temperature in DSC analysis.

situated for PVP I at 197 °C (470 K) is high and low width [25]. In semicrystalline polymers, as is the case of ChA or poly(vinyl alcohol) [21], the molecular motions of chain mobility are restricted and as a consequence the height of glass transition peak might be low. Thus, ChA sample presents an intensive relaxation with maximum at 167 °C (440 K) and small relaxation with maximum at 240 °C (513 K) [25]. DMA studies on ChA films with different degree of deacetylation in the range of 73–100% (Fig. 3) showed that the transition situated at ~167 °C (440 K) for DD = 83 wt.% decreases slowly in magnitude with the decrease of the degree of deacetylation of the ChA sample but the transition temperature increases. As this relaxation was not observed in chitin [26] we followed the suggestion of Blumstein et al. [23] and concluded that the relaxation of ChA at 167 °C (440 K) was mainly caused by the local motions within the amine region of chitosan. Thus, the results shown in Fig. 3 confirmed this conclusion. DMA curves of ChA indicated also a transition at about 240 °C (513 K), very low in magnitude, which we attributed to the glass transition of the amorphous part of ChA. Similar results were observed in our earlier measurements (another type of DMA instrument) [21].

The DMA curves of ChA/PVP I blends are shown in Figs. 4–6. As can be observed, with an increase of the PVP I content in mixture (Figs. 4 and 5) the  $\tan \delta$  is more pronounced. However, all the curves of  $\tan \delta$  of ChA/PVP I blend reveal transition temperatures which

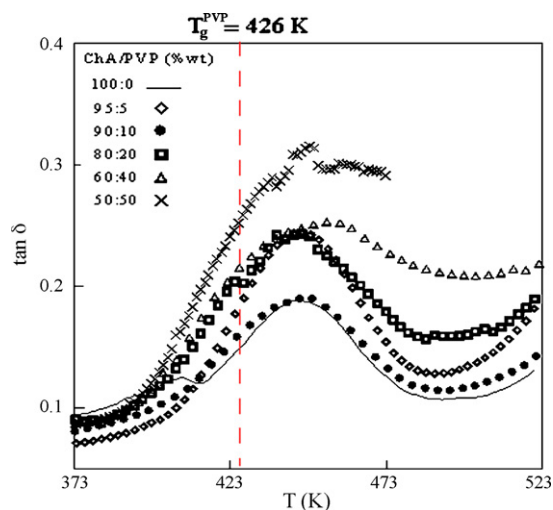


**Fig. 7.** The  $\tan \delta$  thermograms of ChA, PVP II and ChA/PVP II blends (tensile mode).  $T_g^{\text{PVP}}$  evaluated on basis of DSC.

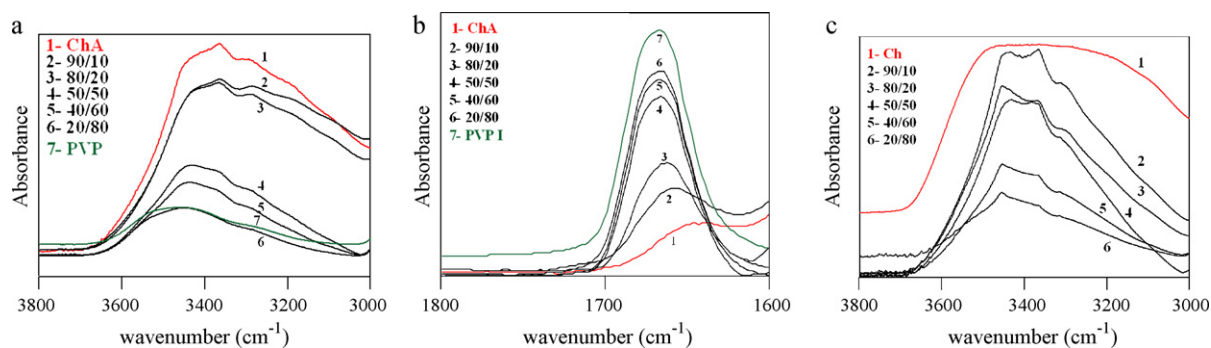


Fig. 8. FTIR spectra of ChA, PVP I and ChA/PVP I blends.

Table 3

Absorption coefficients of hydrogen bonded carbonyl vibrations of ChA/PVP I blends calculated for 25 °C (298 K).

ChA/PVP I (wt.%)	$b$ ( $\times 10^6$ m)	$\rho$ (g/cm <sup>3</sup> )	C=O free		C=O bond		$a_{\text{FCO}}$ (cm <sup>-1</sup> m <sup>2</sup> mol <sup>-1</sup> )	$a_{\text{HBCO}}$ (cm <sup>-1</sup> m <sup>2</sup> mol <sup>-1</sup> )
			$w_{1/2}$	$A_{\text{FCO}}$	$w_{1/2}$	$A_{\text{HBCO}}$		
0:100	10	1166	60	67			640 ± 150	
40:60	10	1225	35	22	56	32		1000 ± 250
50:50	10	1243	22	12	43	37		1000 ± 250
80:20	10	1314	30	10	39	17		2100 ± 500

$b$ : Thickness of the film,  $\rho$ : density,  $w_{1/2}$ : peak widths at half height,  $A_{\text{FCO}}$ : integral intensity of free carbonyl band,  $A_{\text{HBCO}}$ : integral intensity of hydrogen bonded carbonyl band,  $a_{\text{HBCO}}$ : absorption coefficient of hydrogen bonded carbonyl band,  $a_{\text{FCO}}$ : absorption coefficient of the free carbonyl vibration.

roughly correspond to the transition temperatures of the blend components (Fig. 6). It is accepted that such behaviour indicates the lack of miscibility [25]. This conclusion is in the agreement with DSC results presented in this paper (Fig. 6), where the transition temperatures of blends do not change with the blend composition at  $w_{\text{ChA}} > 0.5$ . With lower content of ChA in the blend ( $w_{\text{ChA}} = 0.2$ ) a small shift of transition temperature is observed, suggesting some interaction in the blend (Fig. 5).

As in DSC measurements in the case of ChA/PVP II blends the transition temperature in the amine region of ChA agrees practically with the  $T_g$  of PVP II. As can be seen, the blends at  $w_{\text{PVP}} \leq 0.2$  do not show broader transition. The maximum of  $\tan \delta$  is higher in height with an increase of the PVP II content (Fig. 7). This behaviour indicates partial miscibility of ChA with PVP II. However the DMA determination of the transition temperatures in the investigated system was undoubtedly influenced by the great sensitivity of PVP II to water adsorption, so we could not be sure that the same thermal history leads to the same water content in different blended samples.

### 3.3. FTIR analysis

As both high molecular weight blend components contain proton donor (chitosan OH) and proton acceptor (PVP C=O) groups, they may appear to be miscible, due to the hydrogen bond formation. Thus, the FTIR spectra of film blends, in the carbonyl stretching region of PVP at 1682 cm<sup>-1</sup>, and the hydroxyl stretching bands of chitosan near 3600–3000 cm<sup>-1</sup> have been analyzed. FTIR spectra of films are presented in Fig. 8. As can be observed in Fig. 8a, the

Table 4

The changes of frequency of the carbonyl vibration in the ChA/PVP blends with temperature.

$w_{\text{ChA}}$	ChA/PVP I, $\nu$ (cm <sup>-1</sup> )				ChA/PVP II, $\nu$ (cm <sup>-1</sup> )			
	25 °C	50 °C	100 °C	130 °C	25 °C	50 °C	100 °C	130 °C
0.0	1682 ± 2	1682 ± 2	1682 ± 2	1682 ± 2	1682 ± 2	1682 ± 2	1682 ± 2	1682 ± 2
0.5	1680 ± 2	1680 ± 2	1680 ± 2	1680 ± 2	1682 ± 2	1682 ± 2	1682 ± 2	1682 ± 2
0.6	1680 ± 2	1680 ± 2	1680 ± 2	1680 ± 2	1680 ± 2	1680 ± 2	1680 ± 2	1680 ± 2
0.8					1672 ± 2	1680 ± 2	1680 ± 2	1680 ± 2
0.9	1664 ± 2	1668 ± 2	1676 ± 2	1676 ± 2	1660 ± 2	1660 ± 2	1678 ± 2	1678 ± 2

unblended chitosan acetate provides two major peaks with their maxima at 3428 cm<sup>-1</sup> and 3298 cm<sup>-1</sup>. These peaks are attributed to the –OH and –NH groups, respectively. The –OH band in blends with PVP shifts towards lower frequency and changes its shape. On the other hand, the PVP sample exhibits an absorption peak with its maximum at 1682 cm<sup>-1</sup>, as shown in Fig. 8b. When the polymer is blended with ChA, this absorption signal, which is assigned to the stretching vibration of a C=O group in the pyrrolidone ring, tends to shift to a position of somewhat lower frequency. These observations of frequency shifts for hydroxyl and carbonyl signals may be interpreted as due to the formation of hydrogen bonds between OH groups of ChA and C=O groups of PVP. We noticed similar changes also for chitosan (Ch) in its amine form (Fig. 8c). The shift of hydroxyl groups in Ch/PVP mixture are more pronounced, what indicates that the miscibility of chitosan with PVP is better than in ChA/PVP [27]. Similar direction of changes for Ch/PVP blends was observed by Cao et al. [9] (Ch with  $\bar{M} = 4 \times 10^5$  and DD = 78%, PVP with  $\bar{M} = 4 \times 10^5$ ), Huang et al. [14] (Ch with  $M_r = 400$  kDa and DD = 85%, the molecular weight of PVP was not specified), Tantisaiyakul et al. [15] (Ch with middle viscosity and DD = 75–85%, PVP  $\bar{M} = 1.1 \times 10^6$ ).

In this paper, FTIR analysis was used for quantitative investigation of hydrogen bonds in ChA/PVP blends. An absorption coefficient of hydrogen bonded carbonyl vibration was determined for pure PVP and ChA/PVP blends, by using the Beer–Lambert law [28] and Brisson considerations [29]. Grams Research 2000 was used to decompose the carbonyl band. Pure PVP is characterized in the carbonyl stretching region by a rather broad band at 1682 cm<sup>-1</sup>. This band is a mixed mode containing contributions from the car-

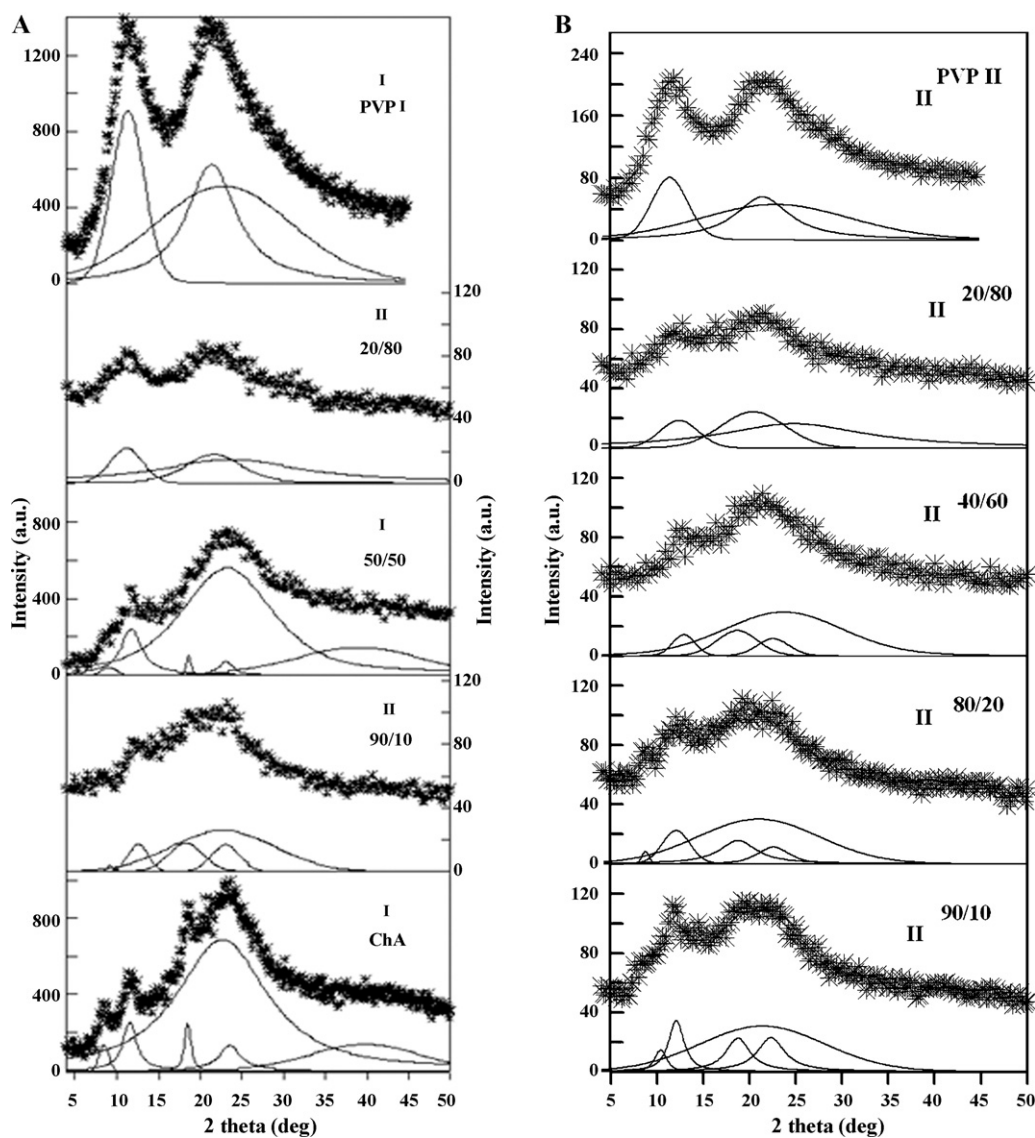


**Fig. 9.** X-ray diffraction patterns of ChA, PVP and their blends: (A) ChA/PVP I; (B) ChA/PVP II; (\*) measured data, (—) adjusted component curves according the Hindeleh and Johnson method [35]. I series – ChA, PVP I and ChA/PVP I blend ( $w_{\text{ChA}}$  of 0.5); II series – ChA/PVP I blends ( $w_{\text{ChA}}$  of 0.9, 0.2) and ChA/PVP II blends ( $w_{\text{ChA}}$  of 0.9, 0.8, 0.4, 0.2).

bonyl stretching and N–C stretching vibrations, which explains the relatively low frequency of this mode compared to the usual carbonyl frequencies. Upon mixing PVP with other polymers, second band is observed at  $1660\text{ cm}^{-1}$  which is readily assigned to hydrogen bonded PVP carbonyl groups [5,30]. Therefore, the vibrations assigned to free and to hydrogen bonded C=O groups attribute to  $1682\text{ cm}^{-1}$  and  $1658\text{ cm}^{-1}$ , respectively. A curve-fitting procedure was used to resolve the absorbance of both carbonyl vibrations. The results of the curve-fitting are listed in Table 3. The absorption coefficient of the free carbonyl vibration is calculated from the pure PVP spectrum as  $640 \pm 150\text{ cm}^{-1}\text{ m}^2\text{ mol}^{-1}$ . It is observed that, with the increase in ChA content, the fraction of hydrogen bonded carbonyl groups increases, especially for  $w_{\text{ChA}} = 0.8$ . This may indicate an involvement of PVP carbonyl groups in the interaction with chitosan acetate.

The influence of temperature (in the range of 298–403K) on the hydrogen bonds in ChA/PVP I and ChA/PVP II blends have been investigated. The obtained results were presented in Table 4. The presented results refer to the bands which have not been resolved to free and to hydrogen bonded C=O groups. As can be seen, the frequency of carbonyl vibration is practical constant with the increase of temperature for the pure PVP and the blends with  $w_{\text{ChA}} \leq 0.8$ .

In the case of blends at  $w_{\text{ChA}} > 0.8$ , the hydrogen bonded carbonyl band shift to higher frequency. The changes of C=O band positions towards higher frequency with the increase of temperature from  $25\text{ }^\circ\text{C}$  to  $100\text{ }^\circ\text{C}$  indicate the weakening of hydrogen bonds in the ChA/PVP blends [27]. The similar change in the range of the temperatures from  $30\text{ }^\circ\text{C}$  to  $60\text{ }^\circ\text{C}$  were observed by Cao et al. [9], who concluded that this phenomenon indicates that the hydrogen-carbonyl hydrogen bonding is reduced with improving the chain motion.

Further increase of temperature up to  $130\text{ }^\circ\text{C}$  does not influence the position of hydrogen bonded carbonyl band of PVP. The shift of carbonyl vibration in the ChA/PVP I blends ( $w_{\text{ChA}} = 0.9$ ) between  $50\text{ }^\circ\text{C}$  and  $100\text{ }^\circ\text{C}$  is lower [ $\Delta\nu(\text{cm}^{-1}) = 8$ ] than the shift for ChA/PVP II [ $\Delta\nu(\text{cm}^{-1}) = 18$ ] of the same composition ( $w_{\text{ChA}} = 0.9$ ). This may indicate that in the ChA/PVP II blends a greater amount of PVP II molecules is involved in hydrogen bonding with ChA.

### 3.4. WAXD

The WAXD pattern of the chitosan acetate film is shown in Fig. 9. Chitosan acetate is a semicrystalline polymer with characteristic peaks at  $2\theta$ :  $8.8^\circ$ ,  $11.6^\circ$ ,  $18.6^\circ$  and  $23.3^\circ$ . The X-ray diffraction

**Table 5**  
Crystallinity of chitosan acetate, PVP and their blends.

	$X_c$ (%)	Series
Blend composition ChA/PVP I		
100:0	12.1 <sub>c</sub>	I
90:10	36 <sub>p</sub>	II
50:50	11.9 <sub>c</sub>	I
20:80	44 <sub>p</sub>	II
0:100	54 <sub>p</sub>	I
Blend composition ChA/PVP II		
100:0	12.1 <sub>c</sub>	I
90:10	46 <sub>p</sub>	II
80:20	35 <sub>p</sub>	II
40:60	28 <sub>p</sub>	II
20:80	46 <sub>p</sub>	II
0:100	54 <sub>p</sub>	II

p: Pseudocrystalline phase, c: crystalline phase.

investigations established five crystalline polymorphs of chitosan [31]. The WAXD measurements of the present investigation show that the X-ray diffraction diagram of chitosan acetate resembles the type I crystal polymorph of chitosan formate [32]. However, the degree of crystallinity of chitosan acetate is low (~12%). As the Bragg angles  $2\theta$  of the investigated chitosan acetate have been found to be similar to the values of  $2\theta$  found by Samuels for chitosan formate [32], it has been assumed that the reflex indexing of the former salt is the same as the latter. On the base of the unit cell dimensions  $a = 7.6 \text{ \AA}$ ,  $b = 10.0 \text{ \AA}$  and with assumption of orthorhombic polymorph ( $\alpha = \beta = \gamma = 90^\circ$ ), the value of  $c = 17.1 \text{ \AA}$  has been calculated [27].

PVP is commonly regarded as an amorphous polymer, though the WAXD pattern of PVP indicates the presence of the pseudocrystalline phase (Fig. 9). The WAXD pattern of PVP shows two halos centered at  $2\theta$ :  $11.3^\circ$ ,  $21.4^\circ$  and  $12.4^\circ$ ,  $20.4^\circ$  for PVP I and PVP II, respectively. The halo at  $\sim 21^\circ$  corresponds to scattering produced by short-range order in the noncrystalline regions, while the more intense maximum at  $\sim 11^\circ$  arise from a pseudocrystalline phase [5,33]. Zekó et al. [34] who investigated the physical aging of poly(vinylpyrrolidone) with low molecular weight under different humidity conditions concluded that a networked structure can be formed, where cross-links by water molecules between different polymeric chains via hydrogen bonds appeared. Thus, the existence of such effects may cause the formation of a pseudocrystalline phase.

The diffractograms of blends were determined in two series. The first was recorded with fresh prepared films. The second series was performed within three weeks. As it is seen, the diffractograms of ChA/PVP I (90:10 and 20:80) and all ChA/PVP II blend films are different from this of 50:50 ChA/PVP I, showing a drastic reduction of the relative WAXD intensities. We suggest that it is the hygroscopic nature of PVP, especially PVP II with relatively low  $\overline{M}_v$  (cf. Table 1), which is responsible for the increase of the amorphous region in the blend, which in turn promotes miscibility of chitosan acetate with PVP. Additionally, the adsorbed water on ChA/PVP II blends may increase the rate of the well known, spontaneous conversion of chitosan acetate to chitosan [36]. In the case of the WAXD pattern of the 50:50 ChA/PVP I blend film (I series), there is no evidence of a mixed-crystal structure that could arise from the interaction of the crystalline and pseudocrystalline phases of the polymeric blend components, because miscibility occurs in the amorphous phase. This conclusion is in agreement with the literature data [8,13].

The crystallinity of samples is presented in Table 5. In the case of blends obtained in the second series the presence of the pseudocrystalline phase is specified. The content of pseudocrystalline phase is greater for ChA/PVP II than ChA/PVP I blends, when compared the mixtures of the same composition (cf. the pair of

blends with  $w_{\text{ChA}} = 0.9$  and the pair of blends with  $w_{\text{ChA}} = 0.2$ ). These results indicate that interactions of chitosan acetate with PVP II (polymer sample of relatively low molecular weight) are more pronounced.

#### 4. Conclusion

The results reported in this paper provide an indication that blends of chitosan acetate of DD = 83% with PVP of different molecular weight (PVP I –  $\overline{M}_r = 9.3 \times 10^5$ , PVP II –  $\overline{M}_r = 2.2 \times 10^4$ ) are poor miscible and that the partial miscibility is driven by hydrogen bond formation between the hydroxyl groups of chitosan and carbonyl groups of PVP. The hydrogen bonding is supported by the shift in the FTIR spectra and the values of absorption coefficient of hydrogen bonded carbonyl band. The shift of hydroxyl groups in chitosan/PVP mixture are more pronounced, what indicates that the miscibility of chitosan with PVP is better than in ChA/PVP. As can be expected the increase of temperature caused the rupture of hydrogen bonds in ChA/PVP blends (at  $w_{\text{ChA}} > 0.8$ ) in the range of 25–100 °C. The DSC measurements of ChA/PVP blends do not show the feature of homogeneous blends (one  $T_g$  value situated between the  $T_g$  values of the polymeric blend components) for chitosan sample of relatively low deacetylation degree (~83%). DMA studies also confirm the poor miscibility of Ch/PVP blends. On the base of the unit cell dimensions  $a = 7.6 \text{ \AA}$ ,  $b = 10.0 \text{ \AA}$  and with assumption of orthorhombic polymorph ( $\alpha = \beta = \gamma = 90^\circ$ ), the value of  $c = 17.1 \text{ \AA}$  has been calculated. The WAXD results reveal that the PVP component is predominantly amorphous, notwithstanding the presence of a phase of low regularity in pure film and in the blends obtained in the second series. In the case of the WAXD pattern of the 50:50 ChA/PVP I blend film (I series), there is no evidence of a mixed-crystal structure that could arise from the interaction of the crystalline and pseudocrystalline phases of the polymeric blend components.

Concluding, in the investigated system of ChA/PVP blends the degree of miscibility between the polymeric components mainly depends on the molecular weight of PVP, moreover on the blend composition and on the moisture content. Thus, the PVP sample with relatively low molecular weight shows partial miscibility with ChA at low content of the polymeric component.

#### References

- [1] P. Molyneux, *Water-Soluble Synthetic Polymers: Properties and Behaviour*, vol. 1, CRS Press Inc., Boca Raton, FL, 1982.
- [2] H. Kagawa, T. Matsui, S. Amemiya, Organic solid photochromism by photoreduction mechanism: viologen embedded in solid polar aprotic polymer matrix, *J. Polym. Sci. Polym. Chem. Ed.* 22 (2) (1984) 383–390.
- [3] G.A.F. Roberts, *Chitin Chemistry*, first ed., Macmillan Press Ltd., London, 1992.
- [4] L.A. Utracki, B.D. Favis, in: P. Nicholas, Cheremisinoff (Eds.), *Handbook of Polymer Science and Technology*, vol. 4, Composites and Speciality Applications, Marcel Dekker Inc., NY, 1989.
- [5] J.F. Masson, R.St.J. Manley, Miscible blends of cellulose and poly(vinylpyrrolidone), *Macromolecules* 24 (1991) 6670–6679.
- [6] Y.M. Lee, S.H. Kim, S.J. Kim, Preparation and characteristics of  $\beta$ -chitin and poly(vinyl alcohol) blend, *Polymer* 37 (1996) 5897–5905.
- [7] J.F. Mano, D. Koniarova, R.L. Reis, Thermal properties of thermoplastic starch/synthetic polymer blends with potential biomedical applicability, *J. Mater. Sci.: Mater. Med.* 14 (2003) 127–135.
- [8] M.T. Qurashi, H.S. Blair, S.J. Allen, Studies on modified chitosan membranes. I. Preparation and characterization, *J. Appl. Polym. Sci.* 46 (1992) 255–261.
- [9] S. Cao, Y. Shi, G. Chen, Blend of chitosan acetate salt with poly(N-vinyl-2-pyrrolidone): interaction between chain-chain, *Polym. Bull.* 41 (1998) 553–559.
- [10] Y. Nishio, T. Koide, Y. Miyashita, N. Kimura, H. Suzuki, Water-soluble polymer blends with partially deacetylated chitin: a miscibility characterization, *J. Polym. Sci. Part B: Polym. Phys.* 37 (1999) 1533–1538.
- [11] L. Fang, S.H. Goh, Miscible chitosan/tertiary amide polymer blends, *J. Appl. Polym. Sci.* 76 (2000) 1785–1790.
- [12] K. Sakurai, T. Maegawa, T. Takahashi, Glass transition temperature of chitosan and miscibility of chitosan/poly(N-vinyl pyrrolidone) blends, *Polymer* 41 (2000) 7051–7056.

- [13] M. Zeng, Z. Feng, C. Xu, Effect of compatibility on the structure of the micro-porous membrane prepared by selective dissolution of chitosan/synthetic polymer blend membrane, *J. Membr. Sci.* 230 (2004) 175–181.
- [14] J.T. Yeh, Ch.L. Chen, K.S. Huang, Y.H. Nien, J.L. Chen, P.Z. Huang, Synthesis, characterization, and application of PVP/chitosan blended polymers, *J. Appl. Polym. Sci.* 101 (2006) 885–891.
- [15] K. Suknuntha, V. Tantishaiyakul, V. Vao-Soongnern, Y. Espidel, T. Cosgrove, Molecular modeling simulation and experimental measurements to characterize chitosan and poly(vinyl pyrrolidone) blend interactions, *J. Polym. Sci. Part B* 46 (2008) 1258–1264.
- [16] G.A.F. Roberts, J.G. Domszy, Determination of the viscometric constants for chitosan, *Int. J. Biol. Macromol.* 4 (1982) 374–377.
- [17] L.C. Cerny, T.E. Helminiak, J.F. Meier, Osmotic pressures of aqueous polyvinylpyrrolidone solutions, *J. Polym. Sci.* 44 (1960) 539–545.
- [18] G.B. Levy, H.P. Frank, Determination of molecular weight of polyvinylpyrrolidone. II, *J. Polym. Sci.* 17 (1955) 247–254.
- [19] T.F.J. Pijers, V.B.F. Mathot, B. Goderis, R.L. Scherrenberg, E.W. van der Vegte, High-speed calorimetry for the study of the kinetics of (de)vitrification, crystallization, and melting of macromolecules, *Macromolecules* 35 (2002) 3601–3613.
- [20] G.Z. Papageorgiou, D.S. Achilias, G.P. Karayannidis, D.N. Bikiaris, Ch. Roupakais, G. Litsardakis, Step-scan TMDSC and high rate DSC study of the multiple melting behavior of poly(1,3-propylene terephthalate), *Eur. Polym. J.* 42 (2006) 434–445.
- [21] K. Lewandowska, Miscibility and thermal stability of poly(vinyl alcohol)/chitosan mixtures, *Thermochim. Acta* 493 (2009) 42–48.
- [22] D.T. Turner, A. Schwartz, The glass transition temperature of poly(*N*-vinyl pyrrolidone) by differential scanning calorimetry, *Polymer* 26 (1985) 757–762.
- [23] J.A. Ratto, C.C. Chen, R.B. Blumstein, Phase behavior study of chitosan/polyamide blends, *J. Appl. Polym. Sci.* 59 (1996) 1451–1461.
- [24] T.G. Fox, *Bull. Am. Phys. Soc.* 1 (1956) 123.
- [25] K. Lewandowska, D.U. Staszewska, M. Bohdanecký, Blend of hydrophilic high molecular weight compounds. Part III. Thermal properties of chitosan acetate/poly(*N*-vinylpyrrolidone) blends, in: H. Struszczyk (Ed.), *Progress on Chemistry and Application of Chitin and Its Derivatives*, Monograph, vol. VI, Polish Chitin Society, Lodz 2000, pp. 63–71.
- [26] K. Ogura, T. Kanamoto, M. Itoh, M. Miyashiro, K. Tanaka, Dynamic mechanical behavior of chitin and chitosan, *Polym. Bull.* 2 (1980) 301–304.
- [27] K. Lewandowska, A. Wojtczak, D.U. Staszewska, Blend of hydrophilic high molecular weight compounds. Part IV. Fourier transform infrared (FTIR) and wide angle X-ray diffraction (WAXD) studies chitosan/poly(*N*-vinylpyrrolidone) blends, in: *Proceedings of the 9th Workshop, New aspects on chemistry and application of chitin and its derivatives*, Krakow, September, 2002.
- [28] J.C. Henniker, *Infrared Spectrometry of Industrial Polymers*, Academic Press, London, 1967, Chap. 7.
- [29] D. Li, J. Brisson, Hydrogen bonds in poly(methyl methacrylate)-poly(4-vinyl phenol) blends: 1. Quantitative analysis using FTi.r. spectroscopy, *Polymer* 39 (1998) 793–800.
- [30] E.J. Moskala, D.F. Varnell, M.M. Coleman, Concerning the miscibility of poly(vinyl phenol) blends—FTi.r. study, *Polymer* 26 (1985) 228–234.
- [31] K. Ogawa, J. Kawada, T. Yui, K. Okuyama, Crystalline behavior of chitosan, *Adv. Chitin Sci.* 4 (2000) 324–329.
- [32] R.J. Samuels, Solid state characterization of the structure of chitosan films, *J. Polym. Sci. Polym. Phys. Ed.* 19 (1981) 1081–1105.
- [33] Y. Nishio, T. Haratani, T. Takahashi, Miscibility and orientation behavior of poly(vinyl alcohol)/poly(vinyl pyrrolidone) blends, *J. Polym. Sci. Part B* 28 (1990) 355–376.
- [34] K. Süvegh, R. Zelkó, Physical aging of poly(vinylpyrrolidone) under different humidity conditions, *Macromolecules* 35 (2002) 795–800.
- [35] A. Hindeleh, D.J. Johnson, The resolution of multipeak data in fibre science, *J. Phys. D: Appl. Phys.* 4 (1971) 259–263.
- [36] S. Demarger-Andre, A. Domard, Chitosan carboxylic acid salts in solution and in the solid state, *Carbohydr. Polym.* 23 (1994) 211–219.